Design of a Broadband Monopole Whip Antenna Based on Trap Circuit Configuration with BWR 1:17.3 for Long Distance Radio Applications

Muddineni Raveendra, Chien Wen Chiu, C. Kohila, and U. Saravanakumar, *Senior Member, IEEE*

***Abstract*— This paper presents the design of a broadband monopole whip antenna for long distance radio communication applications. The design employs an impedance transformer and three parallel trap circuits in the main radiator for broadband performance. The physical limitations of handheld radios limited the whip length to less than 100 cm while preserving operational coverage over the 30-520 MHz frequency range. The trap circuits were integrated on the radiator and coupled to a broadband transmission line transformer (TLT). The constructed TLT was characterized using two calibration techniques: port extension and Through-Reflect-Line (TRL) calibration to extract accurate S-parameters. The measured parameters were then used for full wave simulations. The Genetic Algorithm, interfaced to MATLAB via a visual basic script, was used in HFSS to optimize impedance matching across the entire band (target VSWR < 3.5). Finally, the optimized antenna prototype was fabricated and tested in open field environment by using Vector Network Analyzer (VNA). The measured results confirm the broadband performance of the proposed whip monopole antenna both in impedance and gain requirements from 30 MHz to 520 MHz.**

Link to graphical and video abstracts, and to code: https://latamt.ieeer9.org/index.php/transactions/article/view/11096

***Index Terms*— Broadband antenna, Genetic algorithm, Monopole whip antenna, Transmission line transformer, Trap circuit configuration.**

I. Introduction

THE Portable radios are still a must for wireless communications in military and commercial applications because of their reliability, mobility, and capability of supporting communications over the Very High Frequency (VHF) and Ultra High Frequency (UHF) bands [1]–[3]. Military communication systems (e.g. SINCGARS) need broadband antennas for stable performance across wide operating frequencies, with tight constraints on antenna size, weight, and mechanical robustness. Therefore, the design of electrically small antennas that can simultaneously provide broadband impedance matching, acceptable gain, and small size is still a significant challenge, especially for handheld radio platforms with severely limited ground planes. Broadband monopole antennas with passive loading networks have been widely studied to improve the impedance bandwidth over the VHF /UHF spectrum [11]–[17]. Broadband matching and impedance control have been shown to be effectively realized by parallel inductor-resistor (L/R) loading, trap circuits, transmission-line transformers (TLTs), and genetic algorithm (GA)-based optimization. The use of loading networks and TLTs for significant bandwidth enhancement has been demonstrated in the past [12]–[17]. More recent studies have investigated stepped-slot structures, parasitic loading, sleeve monopoles and reconfigurable RLC matching circuits for further improved broadband performance [32]–[36]. While these approaches have made significant progress, many require large ground planes, have poor low frequency coverage, limited impedance matching over the whole operating band, or use antenna structures that are not desirable for compact handheld radio applications. One major practical problem is that the available ground plane for handheld radio terminals is small and the antenna height is strictly limited, typically less than 1 m. These restrictions lead to very poor radiation efficiency and impedance matching, particularly at lower frequencies where the input impedance of electrically short monopoles is highly reactive. Therefore, achieving ultra-wideband performance under realistic platform constraints is still much harder than under the ideal ground-plane conditions often assumed in previous works.

To address these challenges, this work presents a compact broadband monopole whip antenna with an ultra-wide bandwidth ratio of 1:17.3 over 30-520 MHz. Evolutionary computation has emerged as an important tool in modern wideband design to deal with complex structural boundaries. For example, [37] demonstrated the effectiveness of algorithmic routines by using Particle Swarm Optimization (PSO) to optimize the parameters of a highly compact loaded patch layout. Material boundary constraints also have substantial influences on the terminal impedance characteristics. As confirmed by [38], the variations in the

The associate editor coordinating the review of this manuscript and approving it for publication was Roberto S. Murphy (Corresponding author: *Raveendra Muddineni*).

This work was financially supported by Unication Co., Ltd., Taiwan. The authors also acknowledge the technical support and measurement facilities provided by the company. All authors contributed equally.

Muddineni Raveendra, and C. W. Chiu is with the Department of Electronic Engineering, National Ilan University, Yilan City, Taiwan (e-mails: muddineniravi962tw@gmail.com ,and alexchiu@ems.niu.edu.tw).

C. Kohila is with Electronics and Communication Engineering Department, PSNA College of Engineering and Technology, Dindigul, India (e-mail: kohila.ece2006@psnacet.edu.in).

U. Saravanakumar is with the Electronics and Communication Engineering Department, Muthayammal Engineering College, Namakkal, India (e-mail: saran.usk@gmail.com).

substrate permittivity have a profound effect on return loss profiles in the sub-6 GHz 5G systems, thus highlighting the significance of dielectric choice. The proposed approach is successful in reducing the capacitive mismatch imposed by an electrically small handheld radio chassis by systematically tuning three embedded radiator trap elements on a low cost FR4 substrate. These optimization and material paradigms are mirrored by implementing a Genetic Algorithm (GA) framework.

The proposed antenna employs three optimally located trap circuits along the radiator and a practical ferrite-core 1:4 transmission-line transformer to achieve broadband impedance transformation to a standard 50-Ω system. The proposed TLT is experimentally characterized using Through-Reflect-Line (TRL) calibration for accurate practical implementation unlike many previous studies based on ideal transformer models. Additionally, the passive component values of the trap circuits are optimized using a GA coupled with a full-wave electromagnetic simulator, which allows for the simultaneous optimization of the antenna radiator and matching network while satisfying the stringent dimensional limitations of handheld radio platforms. The main contributions of this work can be summarized as follows: The novelty of the proposed work consists in a simultaneous realization of broadband impedance matching and practical implementation on a compact handheld-radio platform with a severely limited electrical ground plane (0.0049λ x 0.0058λ x 0.014λ) compared to previously reported broadband loaded monopole antennas. The proposed configuration integrates a practical ferrite-core 1:4 transmission-line transformer, whose measured S-parameters are incorporated into the full-wave model, with three passive trap circuits, while a genetic-algorithm framework is used to optimize the passive loading and radiator dimensions. The proposed antenna is experimentally verified on the compact radio chassis over 30-520 MHz with a BWR of 1:17.3. The proposed design differs from previously reported broadband loaded monopoles in that it combines wideband operation with demonstrated compatibility with the limited ground-plane condition of compact handheld radios as summarized in Table. II. The rest of this paper is organized as follows. The proposed monopole whip antenna configuration and the integration of the trap circuits with the handheld radio platform are discussed in Section II. The design, characterization and integration of the ferrite-core transmission line transformer is presented in Section III. In Section IV, the genetic-algorithm optimization process is described, and the simulated and measured antenna performance, including VSWR, gain, and radiation characteristics, is discussed. Section V concludes the paper and summarizes the main findings and possible future improvement directions.

II. Proposed Antenna Design

A monopole antenna is a type of radio antenna that consists of a linear, rod-shaped conductor placed vertically above a conductive surface, commonly referred to as the ground plane. The proposed design uses a monopole whip antenna for its structural flexibility which enables it to be collapsed for easy handling in mobile applications. The proposed wideband monopole whip antenna initial design was formulated using High Frequency Structure Simulator (HFSS) which is an electromagnetic simulation software based on the finite element method (FEM) . In this section, the complete design procedure of integration of monopole whip antenna into a portable device is described. The schematic diagram of the proposed antenna is shown in Fig. 1.

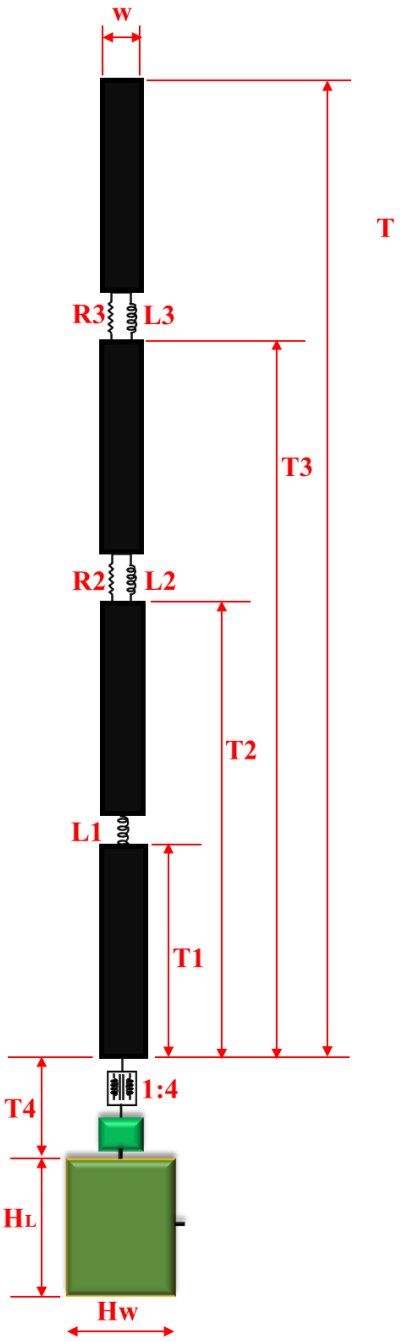


Fig. 1. The schematic diagram of the proposed antenna (T=978 mm, T1=127 mm, T2=419 mm, T3=556 mm, T4=59 mm, H_L =140 mm, W=12.6 mm, H_W = 58 mm).

The antenna radiator was T = 97.80 cm in length and W = 12.6 mm in width consisting of copper whip. The radiator was cut carefully to make three slots at 127 mm, 419 mm and 556 mm from the bottom. In the simulation, the first trap circuit at the 127 mm slot was modeled as an inductor with RLC lumped circuit boundary conditions. The second and third positions

were likewise modeled with parallel resistor-inductor configurations, utilizing RLC boundary conditions as well. To accurately simulate the transmission line transformer (TLT) in HFSS, the S-parameter (S_2P) file extracted from the TLT measurements was used in the model of the proposed monopole whip antenna. Also, an inverted L-shaped printed antenna for GPS applications on a FR4 substrate (relative dielectric constant εr=4.4) was integrated to the system (details are not disclosed due to copyright restrictions). Conductive pathways exist on the top and bottom surfaces of the FR4 substrate. One terminal of the upper conductor trace is connected to a 50 Ω input impedance port while the other terminal is connected to the behavioral model of the transmission line transformer. The lower conductor trace is connected to the ground plane. A rectangular copper chassis was used as the handset ground plane, having dimensions of 4.9 cm length, 5.8 cm width, and 14 cm height. The metallic casing acts as the ground plane for the antenna and also as the mechanical support for the proposed monopole whip antenna inside the mobile device.

The limited ground plane (0.0049λ x 0.0058λ x 0.014λ) and the separate trap circuits have a strong effect on the suggested monopole whip antenna impedance properties. In our previous work [39], we have shown that reducing the ground-plane size improved the capacitive nature of the antenna input impedance and the resonant frequencies, which made it more difficult to match the impedance at lower frequencies. With the present configuration, the device chassis is a basic part of the antenna system, not an ideal infinite ground plane. The three trap circuits are employed for controlling the effective electrical length of the radiator at different frequency ranges, to adjust the resultant impedance characteristics. In the lower and middle frequency ranges the current path and response are mainly determined by the inductive components L1, L2 and L3 while the resistive components R2 and R3 reduce current in selected portions of the radiator at the higher frequencies, thus reducing the active electrical length considerably. Thus, the integrated trap configuration makes it possible to selectively excite radiator sections according to the operating frequency, thus improving the broadband impedance performance of the proposed antenna. Ground-plane dependence and specific trap-element sensitivities have been studied extensively in [39]. Thus, this work is not a repetition of previously published parametric results but rather a focus on the optimized configuration and its experimental verification.

III. Utilization of Transmission Line Transformer

The practical ferrite core transmission line transformer was tested for efficacy from 30 MHz to 520 MHz using an HP-5071B Vector Network Analyzer (VNA). This transformer is manufactured by Unication Co., Ltd, which is designed to meet broadband specifications for this frequency range as shown in Fig. 2(a) and Fig. 2(b). As mentioned earlier, broadband impedance matching requires transmission line transformers. However, the transformer is complex and it is difficult to simulate it exactly in HFSS. Thus, the transformer was characterized at the outside and the corresponding S-parameter (S_2P) file was imported in the HFSS simulation. Two calibration techniques were used for the S-parameter measurement of the ferrite core transformer. One is the standard two-port calibration with port extension and the other is the TRL (Through-Reflection-Line) calibration to de-embed the reference planes with high accuracy.

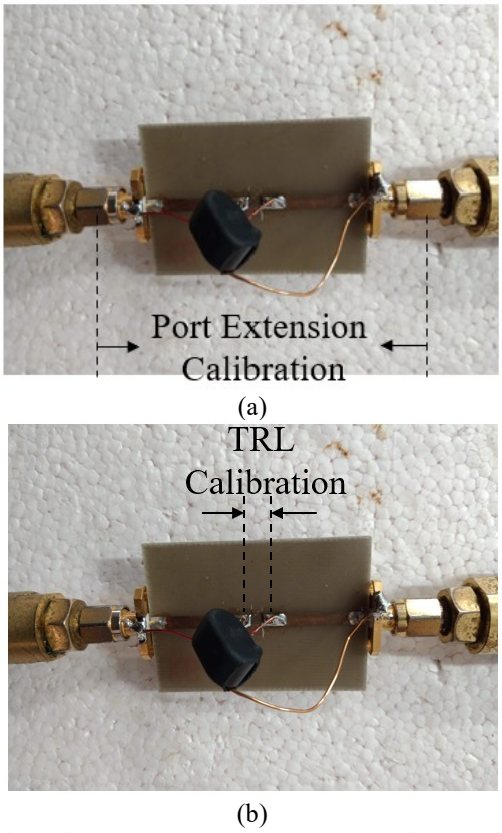


Fig. 2. The utilization of ferrite core transmission line transformer for broadband impedance matching and its measurement set up under (a) port extension method and (b) TRL calibration method.

The transmission line transformer was initially tested with standard 50 Ω input and output connectors. However, it was not easy to connect the transformer's output terminal directly to a 200 Ω load, as there were no coaxial cables and connectors available with a 200 Ω rating. Therefore, the ferrite core transmission line transformer was tested with 50Ω load configuration. The recorded S-parameter (S_2P) file was then stored and loaded into the Advanced Design System (ADS) software where a 200Ω load was simulated to accurately determine the insertion loss of the transmission line transformer. As per Fig. 3(a), and Fig. 3(b), the $|S_{11}|$ and $|S_{12}|$ performance was not satisfactory, as the transformer was connected to a 50 Ω load while it is designed to transform a 200 Ω load to 50 Ω. Therefore, the S-parameter file of the ferrite core TLT was replaced by the simulated load terminal of 200 Ω. In this case, the $|S_{11}|$ impedance matching was greatly improved at the lower frequency region (see Fig. 4(a)) but gradually degraded at higher frequencies with the increase in the inductive effects. The insertion loss was found to be sufficient in the operational frequency spectrum of 30 MHz to 520 MHz. This shows the effective operation of 1:4 ferrite core transmission line transformer. The insertion loss achieved by TRL calibration is compared with that from port extension (two-port calibration) in Fig. 4(b). For a 200 Ω load, the insertion loss (S_{12}) obtained by the TRL calibration was better

than −2.5 dB from 30 MHz to 300 MHz and worse than -3.8 dB from 300 MHz to 520 MHz. The transmission efficiency of the transformer decreases at higher frequencies due to increased losses in the ferrite material, especially in the UHF range (380 MHz to 520 MHz) leading to insertion losses between −3 dB and −4 dB.

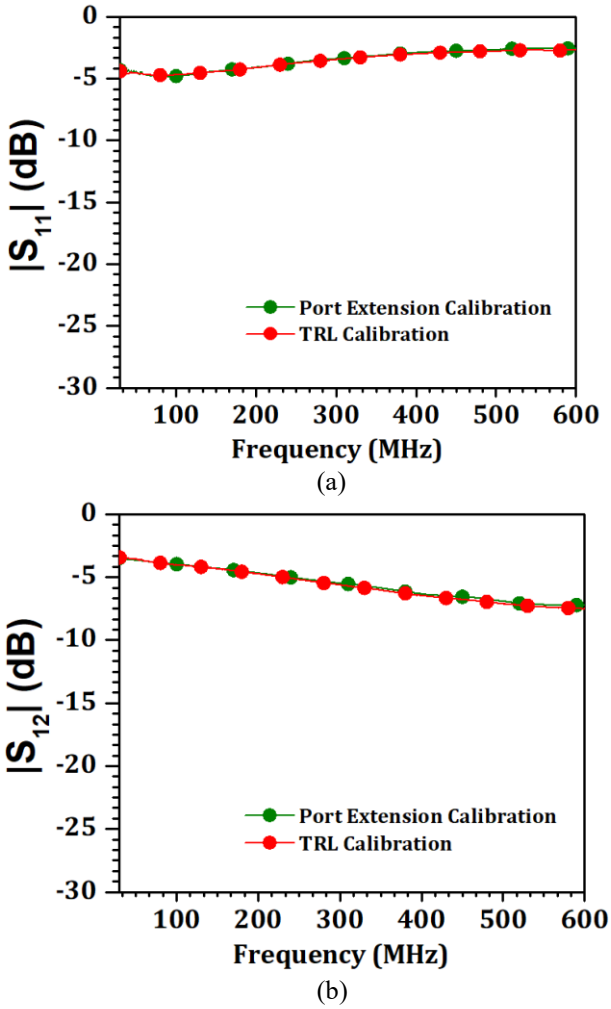


Fig. 3. Measured (a) S_{11} and (b) S_{12} of the transmission line transformer under the 50 Ω load terminal.

The physical construction of the proposed antenna is shown in Fig. 5(a) with the experimental set up. To determine the role of the transmission-line transformer (TLT) in broadband impedance matching, the trap circuits were temporarily replaced by zero-ohm links to analyze the TLT separately as shown in Fig. 5(b). The input impedance of the ferrite-core TLT and without it was compared in the Smith chart in the range of frequencies 30-200 MHz. The impedance trajectory was dominated by capacitive reactance, hence poor impedance matching without TLT. The impedance locus shifted to the inductive region after TLT, signifying a more balanced blend of inductive and capacitive reactance throughout the operating band. Such a behavior shows that the ferrite-core TLT is very effective to transform the highly reactive antenna impedance to a value more compatible with a standard 50-Ω system, thereby improving broadband impedance matching.

The accuracy of the proposed antenna model was further verified by comparing the simulated and measured return losses after integrating the TLT as shown in Fig. 6. The measured results are in good agreement with the simulated response over the operating band, which validates the electromagnetic model. Any minor differences between the two results are mainly due to the insertion loss of the practical ferrite core TLT, manufacturing tolerance and component parasitic that are not fully modeled in the simulation. However, the measured results prove the effectiveness of the proposed impedance-matching approach. Then the full monopole antenna was tested with the optimized trap-circuit configuration along with the ferrite-core TLT. Fig. 7 shows the simulated reflection coefficient of the proposed monopole antenna using the initial trap-circuit component values before GA optimization. Measurements were made both inside and outside an anechoic chamber to reduce the effects of the near-field at the lower VHF frequencies. The simulated and measured return losses of the complete antenna are compared in Fig. 7.

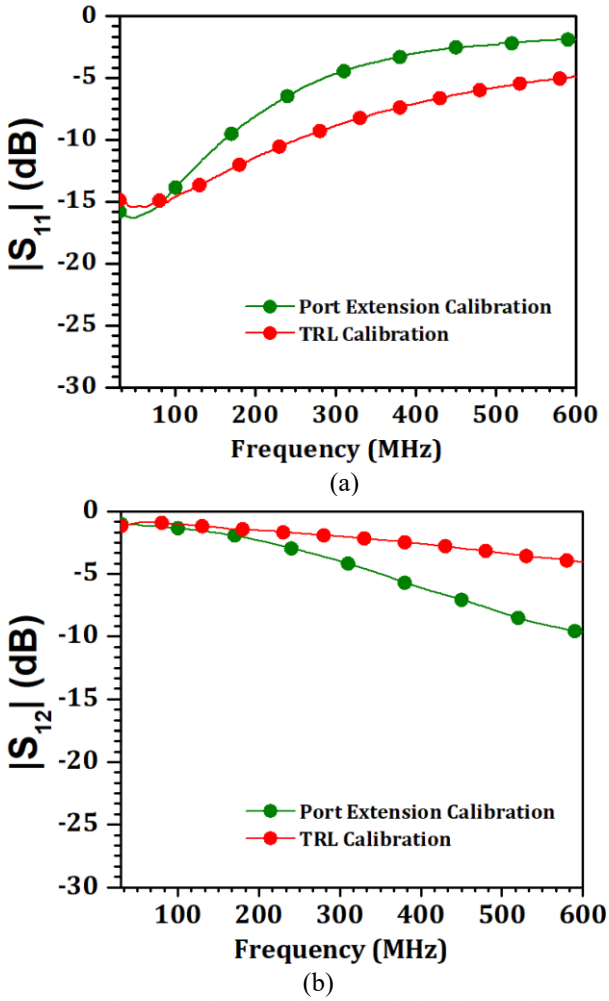


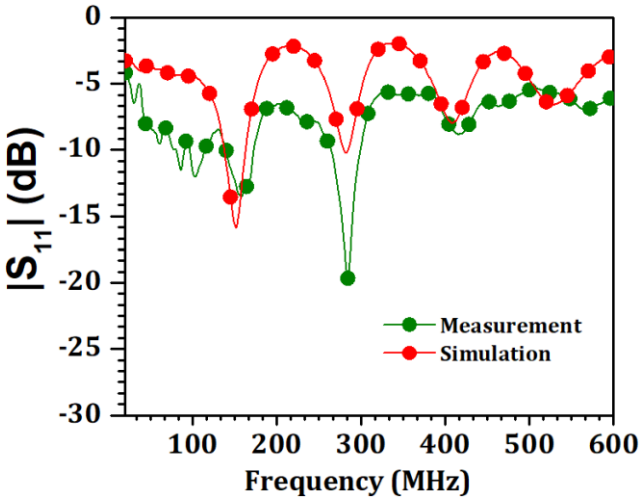
Fig. 4. Measured (a) S_{11} and (b) S_{12} of the transmission line transformer under the 200 Ω load terminal.

The overall response trends are in good agreement but some degradation of the measured return loss is observed at higher frequencies. The mismatch is most likely due to the fabrication tolerances, the uncertainties in the position of the components, the conductor losses and the frequency dependent losses of the

ferrite-core transformer. These practical effects do not influence the measured results which demonstrate that the proposed antenna gives a broad band impedance matching over the desired operating frequency band.



(a)



(b)

Fig. 5. The proposed antenna: (a) physical monopole antenna setup and (b) its reflection coefficient with the TLT integrated while L1, L2, L3, R2, and R3 replace with 0 Ω.

The resonant frequency in the low VHF band can be modulated from 86.70 MHz to 75.10 MHz by changing the values of Lm from 0.6 µH to 3.2 µH. The change in resonance frequency over the low VHF band due to changes in Lm is approximately 11.60 MHz. Similarly, Lm can regulate the operation frequency in the mid VHF spectrum from 174.42 MHz to 157.02 MHz for values between 0.6 µH and 3.2 µH. It was found that the change of resonance frequency in the VHF range due to change of Lm is about 17.40 MHz. The tuning range can be further increased by increasing the value of Lm. However, the study shows that the performance of impedance matching degrades significantly with the increase of Lm at the lower part of the VHF range. For the UHF band, the resonant frequency was tuned from 407.87 MHz to 418.02 MHz when Lm was varied from 0.6 µH to 3.2 µH, with a tuning range of about 10.15 MHz. Furthermore, the UHF band return loss effectiveness gets better with the increase of Lm.

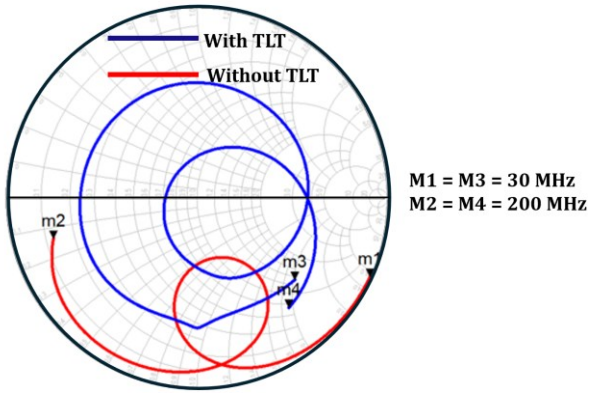


Fig. 6. The behavior of the impedance matching in the presence of TLT but without TLT.

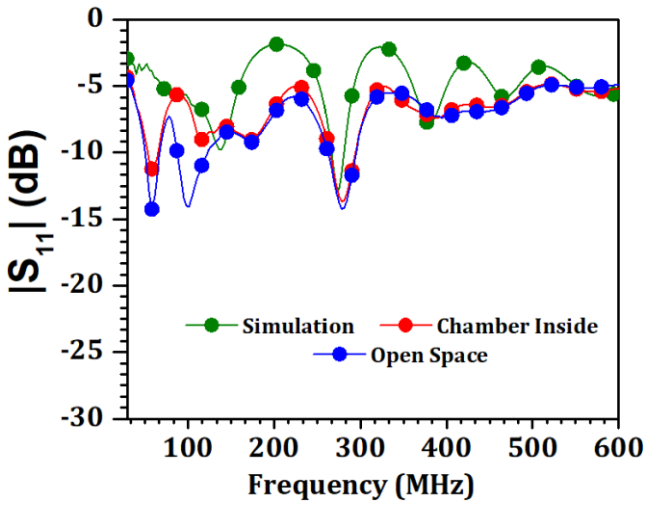


Fig. 7. The reflection co-efficient of the proposed monopole antenna in the presence of TLT while L1 = 3nH, L2 = 50nH, L3 = 75 nH, R2 = 1.5k Ω, and R3 = 1.5 k Ω replace with their initial values.

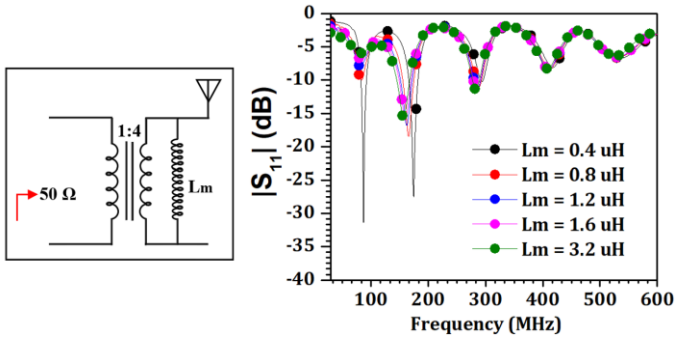


Fig. 8. The schematic diagram for the implementation of the shunt inductor (L_m) and its influence on the $|S_{11}|$.

IV. Results and Discussion

Initially, a visual basic script was used to interface MATLAB with HFSS to automate the optimization process. TABLE I summarizes the lower and upper bounds of the design

variables involved in the optimization. The genetic algorithm (GA) uses binary chromosomes to represent the design variables which are then converted to their corresponding real valued parameters within the predefined optimization limits. Following the methodology described in [26] and [28], the conversion is performed using

$$P = p_{min} + \left(\frac{p_{max} - p_{min}}{2^{N^p}-1}\right)\left(\sum_{n=0}^{N^p-1} b_N^P \, 2^n\right) \quad (1)$$

Where "P" is the design parameter, p_{min} and p_{max} are the upper and lower bounds, respectively, N^p is the number of binary bits assigned to each parameter, and b_N^P is the value of the n^{th} binary gene. Then the decoded parameters are passed from MATLAB to HFSS via the Visual Basic interface to perform full-wave electromagnetic simulations and obtain the corresponding antenna input impedance. The obtained impedance data are then used in MATLAB to calculate the magnitude of the reflection coefficient at each frequency point as

$$|\Gamma(f_i)|_{calculated} = \frac{z_{in} - z_0}{z_{in} + z_0} \quad (2)$$

Where (Zin) is the impedance at the antenna input, (Z_0) is the characteristic impedance of the feeding system (50Ω) and (f_i) is the i^{th} frequency point in the simulation sweep. The impedance-matching performance of the proposed antenna is evaluated from the calculated reflection-coefficient magnitude using the following fitness function:

$$F = \sum_{i=1}^{N} \{w_i \, (|\Gamma(f_i)|_{Calculated} - |\Gamma(f_i)|_{Desired})^2\} \quad (3)$$

Where (F) is the fitness error, $|\Gamma(f_i)|_{Calculated}$ and $|\Gamma(f_i)|_{Desired}$ are the calculated and desired reflection coefficient magnitudes respectively, w_i is the weighting factor applied to the i^{th} frequency point and (N) is the total number of frequency points taken into account in the optimization. The desired reflection-coefficient magnitude is 0.5, corresponding to a voltage standing wave ratio (VSWR) of 3. In the fitness evaluation the error is calculated only for the frequency points whose reflection-coefficient magnitude is above the given threshold, the other points are neglected. The GA iteratively minimizes this error in order to improve the impedance matching over the operating frequency range. The frequency range of 30 MHz to 200 MHz was chosen for the first stage of optimization taking into account the transmission line transformer experimentally characterized in the antenna model. The target was a reflection-coefficient magnitude less than 0.5 or a VSWR less than 3. This criterion provides a practical compromise between broadband impedance match and the physical limitations of the proposed antenna. At low frequencies of operation, the electrically short monopole has a large capacitive reactance which makes impedance matching difficult. Thus, the goal of GA is more to realize a large impedance bandwidth rather than a stricter matching requirement at individual frequency points. The optimization was done with population size 20, tournament selection, crossover rate 0.8 and mutation rate 0.01. The optimization converged after 45 generations, with a final error of approximately 0.96 %, as shown in Fig. 9. To evaluate the convergence behavior, the mean fitness error for each generation was calculated by averaging the individual fitness errors over the population, as expressed by

$$\text{Mean} = \frac{\text{Sum of individual errors for a perticular generation}}{\text{Popoluation size}} \quad (4)$$

Where the numerator is the sum of the fitness errors of the individuals in a particular generation, and the determinant is the population size. Furthermore, the progress of the optimization was evaluated by monitoring the best fitness error obtained at each generation. Mean and best fitness errors were illustrated using the following penalty-value expression described in [31], [39]:

$$\text{Penalty value} = [\text{Mean}, \text{Error}] \quad (5)$$

Where Mean is the average fitness error of the population and Error is the best fitness error achieved in the corresponding generation. At successive generations these quantities were calculated to check the convergence of the optimization process. In our previous paper [39], we presented a complete step-by-step procedure for integrating MATLAB and HFSS.

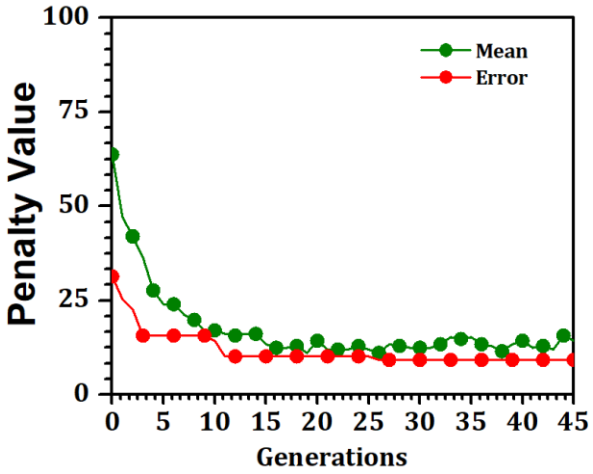


Fig. 9. The error function response during the 30 MHz to 200 MHz optimization process using GA.

Fig. 10 shows the optimized VSWR which is less than 3 for the entire frequency range of 36 MHz to 200 MHz and less than 3.5 for the lower frequency range of 30 MHz to 35 MHz. The design criteria allow a VSWR below 3.5 to be acceptable in the near HF spectrum. The final values of the passive components after optimization are shown in TABLE I. For the improvement of the antenna efficacy on the frequency spectrum of 100 MHz-520 MHz the simulation sweep range was changed accordingly. In this stage an optimal transmission line transformer model was used to speed up the optimization procedure. To assist with the matching, a shunt inductor Lm of 0.3 μH was added at the feed point. Lm can be considered variable, but fixing it reduces the computational time for the large number of optimization parameters. The aim of the optimization was to obtain a reflection coefficient $|\Gamma| < 0.5$ (VSWR < 3) over the entire spectrum from 100 MHz to 520 MHz. The 6th iteration is shown in Fig. 11 and the objective was achieved without error.

The improved VSWR shown in Fig. 12. Looking at Fig. 12, the VSWR was maintained below 3 (equivalent to $|S_{11}| < -6$ dB) with a much more uniform curve. This is because Lm was introduced at the feed point. Finally, the monopole whip antenna was evaluated using a practical ferrite core transmission line transformer (TLT). The final passive components, refined under best TLT conditions, were directly modified as L1=3.6nH, L2=1000nH, L3=470nH, R2=100Ω, R3=200Ω, T1=148.462mm, T2=499.121mm, T3=904.081mm and calibrated during testing for minor adjustments. Fig. 13 shows the measured voltage standing wave ratio (VSWR) which was below 3.5 in the low VHF band and below 3 in mid VHF and UHF bands. Fig. 14(a), Fig. 14(b), and Fig. 14(c) shows the measured realized gain of the proposed monopole antenna in the low VHF, mid VHF, and UHF frequency bands, respectively. The measured gain varies from -32.58 dBi to -4.52 dBi in the low VHF band, -9.83 dBi to 4.39 dBi in the mid VHF band and -15.24 dBi to -4.74 dBi in the UHF band. The relatively low gain at the lower end of the VHF band is expected as the antenna is electrically short at these frequencies and is operating on a small handset ground plane. Similarly, the loss in the UHF band gain is mainly due to the ferrite core TLT.

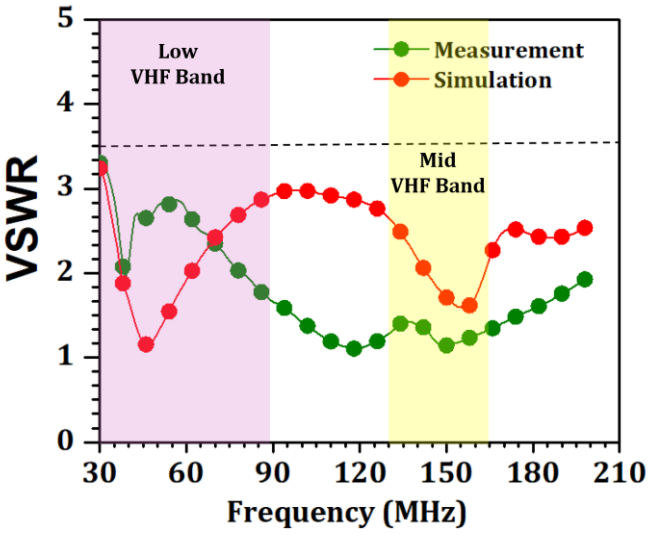


Fig. 10. The optimized VSWR from 30 MHz to 200 MHz using a genetic algorithm.

The antenna gain is not flat but the overall transmitting performance is determined by the effective isotropic radiated power (EIRP) of the whole RF front-end rather than the antenna gain alone. The sponsors' company developed the transmitter composed of two cascaded power amplifiers, providing a gain of about 15 dB each. The RF chain provides a total gain of about 30 dB. Increasing the transmitter output power does not change the intrinsic gain or the radiation efficiency of the antenna. However, it can increase the overall effective isotropic radiated power (EIRP) of the transmitter-antenna system. Therefore, if the antenna gain is limited by the physical dimensions and the operating frequency, the increase of the available output power of the transmitter may be used to achieve the required EIRP level, within the applicable transmitter power and regulatory limits.

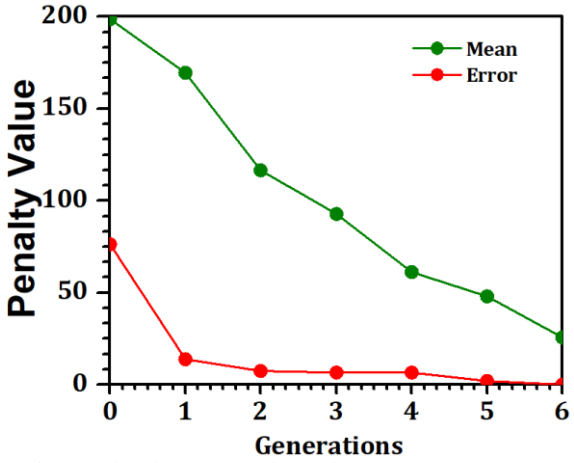


Fig. 11. The error function response during the 100 MHz to 520 MHz optimization process.

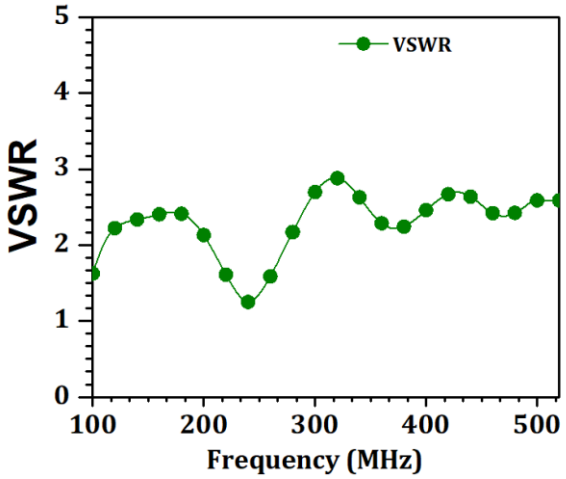


Fig. 12. The optimized VSWR from 100 MHz to 520 MHz using a genetic algorithm.

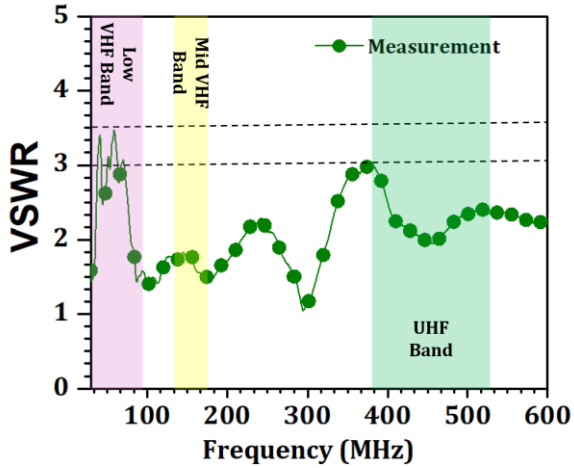


Fig. 13. The measured VSWR from 30 MHz to 520MHz.

As per TABLE III, the estimated EIRP is based on the measured antenna gain and the transmitter output power. The estimated EIRP ranges from about -6.58 dBm to 21.48 dBm in the low VHF band, 16.17 dBm to 30.39 dBm in the mid VHF band, and 10.76 dBm to 21.26 dBm in the UHF band.

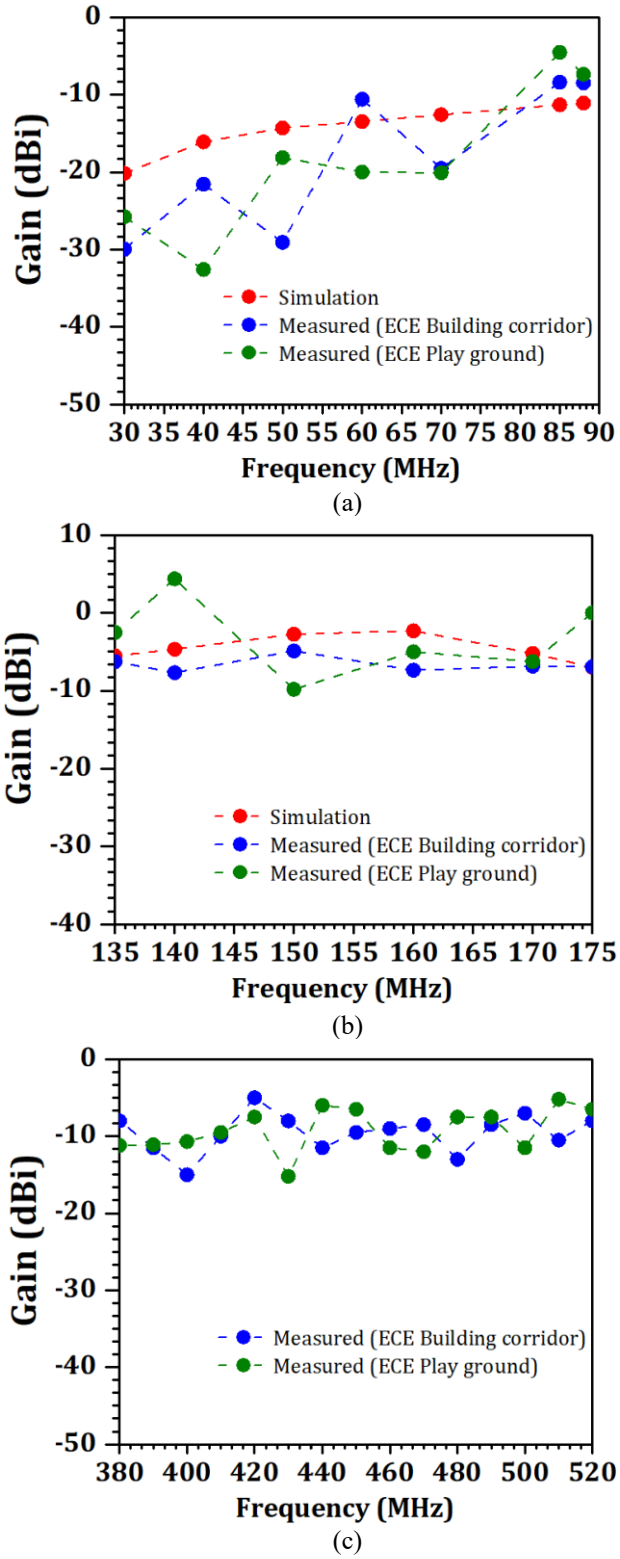


Fig. 14. The peak gain of the proposed antenna (a) low band, (b) mid band, and (c) high band.

The results show that, when incorporated into the intended transmitter architecture, the proposed antenna provides enough radiated power to achieve reliable performance over the entire 30–520 MHz frequency range, despite the inherent gain variation of electrically short broadband antennas.

The antenna radiation patterns at the resonant frequency of 100 MHz in E-plane and H-plane are modeled as shown in Fig. 15(a) and Fig. 15(b) respectively. The practical hand set ground has marginal effect on the radiation characteristics. This is observed in Fig. 15(a) and Fig. 15(b) when the ideal horizontal ground plane is replaced. The E-plane and H-plane patterns are not significantly affected. This confirms the proposed antenna can operate efficiently on a compact handheld platform, without the need of an electrically large ground plane. This is an important advantage over many previously reported broadband monopole antennas, whose performance is highly dependent on large ground planes. The negative gain in the UHF band is mainly a result of the loss of the ferrite core of the TLT. Designing or using a low-loss TLT at higher frequency can achieve such a loss reduction. However, a high-power amplifier in the transceiver can compensate for about 4 dB attenuation due to TLT in the UHF spectrum. The functional antenna design fulfills the specifications requirements for the proposed monopole whip antenna model in the frequency range of 30 MHz to 520 MHz as reported in the above stated study. The proposed antenna is highly miniaturized with a size less than $\lambda/10$, which is much smaller than the antennas reported in the literature. Its compact design allows the antenna to be easily transported or folded onto the whip as desired. A major challenge overcome by this work is the performance demonstrated in all presented metrics, even with the limited electrical ground plane imposed by the radio's configuration. Finally, TABLE II shows the compatibility of handheld radios with the existing antennas. The existing antennas were designed for operation in low VHF, mid VHF and UHF bands. The practical losses of the ferrite-core transmission line transformer (TLT) directly affect the overall antenna efficiency and realized gain in a frequency-dependent manner.

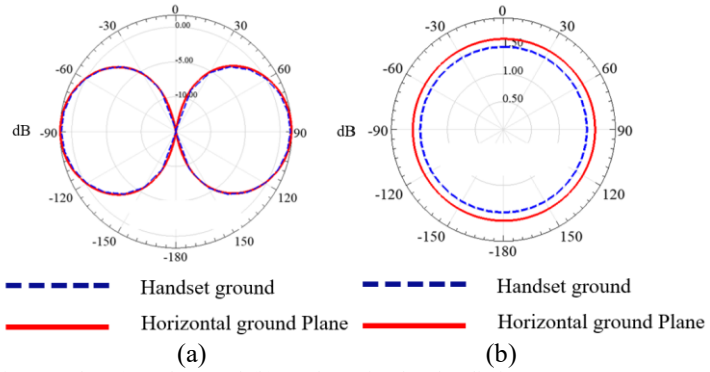


Fig. 15. The (a) E-plane and (b) H-plane simulated radiation patterns at 100 MHz.

The ferrite core has a high permeability at the lower VHF frequencies (30-88 MHz) which makes possible the efficient linking of the magnetic flux and translation of the impedance with a tolerable insertion loss. However, as the operating frequency is increased to the higher UHF band (380-520 MHz), the core material suffers significant degradation due to increased magnetic core losses (hysteresis and eddy current losses) and frequency-dependent copper losses in the windings. The TRL calibration profile shows the insertion loss penalty of −3 dB to −4 dB due to the core saturation and loss of effective permeability.

TABLE I
THE OPTIMIZED PASSIVE TRAP CIRCUIT ELEMENTS VALUES USING GA

		30 MHz -200 MHz				100 MHz -520 MHz			
S.No	**Variable parameters**	**p_{min}**	**p_{max}**	**Optimized value**	**Experiment value**	**p_{min}**	**p_{max}**	**Optimized value**	**Experiment value**
1	L1 (nH)	0.1	1000	859.355	820	0.1	1000	3.27429	3.6
2	L2 (nH)	0.1	1000	944.572	1000	0.1	1000	968.257	1000
3	L3 (nH)	0.1	1000	994.384	1200	0.1	900	421.792	470
4	R2 (Ω)	100	2000	203.004	200	100	2000	119.951	100
5	R3 (Ω)	100	2000	318.071	330	100	2000	149.182	200
6	T1 (mm)	60	150	98.7106	98.7106	60	150	148.462	148.462
7	T2 (mm)	100	350	140.74	140.74	100	550	499.121	499.121
8	T3 (mm)	100	920	159.397	159.397	100	920	904.081	904.081

TABLE II
PERFORMANCES OF BWR COMPARISON TABLE BASED ON ELECTRICAL GROUND COMPATIBILITY

Ref. No	**Antenna Type**	**Matching Technique**	**BWR**	**Remarks**
[12]	Monopole Wire Antenna	LC	1:05	No discussion about grounding effect
[13]	Monopole Wire Antenna	RL	1:20	Not compatible for compact radios due to large ground plane
[14]	Monopole antenna	RLC	1:17.3	Not compatible for compact radios due to large ground plane
[15]	Monopole Wire Antenna	RLC	1:17	No discussion about grounding effect
[25]	Broadband Monopole	RL	1:20	Not compatible for compact radios due to large ground plane
[26]	Loaded Dipole antenna	LC	1:40	Not compatible for compact radios due to large ground plane
[27]	Monopole antenna	Stubs loading	NA	No discussion about grounding effect
[29]	Monopole antenna	C	1:03	Not compatible for compact radios due to large ground plane
[30]	Slim Monopole antenna	LC	02:00.0	Applicable for compact radio applications
[32]	Broadband reconfigurable antenna	Stepped slots loading	01:04.3	Not compatible for compact handheld radios
[33]	Baseline moisturized antenna	Active RLC	1: 1.2	Not compatible for compact handheld radios
[34]	Slim Monopole antenna	Parasitic Loading	1: 4.31	Applicable for compact radio applications
[35]	Sleeve Monopole Antenna	Choke structure	1: 3.95	Not compatible for compact handheld radios
[36]	Reconfigurable UWB Antenna	RLC	1: 3.87	Not compatible for compact handheld radios
This paper	Whip Monopole Antenna	RL	1:17.3	Applicable for compact radio applications

These core dissipations reduce the input power before it reaches the radiator, thus reducing the measured realized gain to -15.24 dBi at the lower end of the UHF spectrum, as the realized gain is proportional to the radiation efficiency. A band-bypassing circuit configuration or low-loss, high-frequency core material may be used to decouple the TLT during UHF transmission to alleviate these practical limitations in future deployments.

V. CONCLUSION

This work presented the design, optimization, and experimental validation of a broadband monopole whip antenna operating from 30 MHz to 520 MHz for handheld radio applications.

TABLE III
LINK BUDGET OF THE PROPOSED ANTENNA

Band	Worst / Best	Transceiver output (dBm)	B.P.F (dB)	Trace Loss (dB)	Cable Loss (dB)	Antenna Gain (dBi)	EIRP (dBm)
Low VHF	Worst case	30	-3	-0.5	-0.5	-32.58	-6.58
	Best case	30	-3	-0.5	-0.5	-4.52	21.48
Mid VHF	Worst case	30	-3	-0.5	-0.5	-9.83	16.17
	Best case	30	-3	-0.5	-0.5	4.39	30.39
UHF	Worst case	30	-3	-0.5	-0.5	-15.24	10.76
	Best case	30	-3	-0.5	-0.5	-4.74	21.26

A hybrid approach was adopted using trap circuits, a practical ferrite-core transmission line transformer (TLT), and a shunt inductor (L_m) to ensure broadband impedance matching across the Low-VHF (30–88 MHz), Mid-VHF (135–175 MHz), and UHF (380–520 MHz) bands. The ferrite-core TLT was characterized using a TRL calibration method and validated through measurements of its impedance performance under both 50 Ω and 200 Ω load conditions. Results confirmed that the TLT effectively transforms high impedance to low impedance, especially in the 30–88 MHz range, making it suitable for low-frequency broadband applications. The Smith chart analysis further demonstrated significant improvements in impedance matching after integrating the TLT. Genetic algorithm (GA) optimization was employed for passive component tuning, achieving a VSWR < 3.5 from 30–35 MHz and < 3 from 36–520 MHz. The return loss improved correspondingly with the optimized values, and the effect of the shunt inductor (L_m) was shown to influence both impedance matching and resonance frequency shifting across VHF and UHF bands. In the gain performance evaluation, the peak measured gain was approximately -4.52 dBi in the low VHF band, 4.39 dBi in the mid VHF band, and -4.74 dBi in the UHF band under a very small electrical ground plane—a core challenge of this research. The negative gain in the UHF band was attributed to ferrite losses in the TLT. To address this, a future TLT design with reduced loss is proposed, which is expected to enhance UHF gain performance by approximately 4 dB. A comparative study with existing literature, summarized in TABLE II, highlights the advantages of the proposed antenna in terms of compactness (< λ/10), broadband coverage, and practical deployability. The design effectively operates over a broad frequency range using a minimal ground plane, addressing a critical challenge in handheld radio antenna design and proving its suitability for modern transceiver systems.

REFERENCES

[1] E. Garcia, A. Andujar, and J. Anguera, "Overview of reconfigurable antenna systems for IoT devices," *Electronics*, vol. 13, no. 20, Art. no. 3988, 2024, doi: 10.3390/electronics13203988.

[2] H. Chen and K. M. Luk, "Detection capability enhanced biosensor antenna for portable electromagnetic stroke diagnostic systems," *IEEE Trans. Biomed. Circuits Syst.*, vol. 18, no. 1, pp. 145–159, Feb. 2024, doi: 10.1109/TBCAS.2023.3313732.

[3] T. Taga and K. Tsunekawa, "Performance Analysis of a Built-In Planar InvertedFAntenna for 800 MHz Band Portable Radio Units," in IEEE Journal on Selected Areas in Communications, vol. 5, no. 5, pp. 921-929, June 1987, doi: 10.1109/JSAC.1987.1146593.

[4] J. Louro, L. Nunes, F. Barradas, P. Cabral, and J. C. Pedro, "The impact of a taper impedance transformation on the TRL de-embedding error," *IEEE J. Microwaves*, early access, 2024, doi: 10.1109/JMW.2024.3405018.

[5] Y. Feng, X.-C. Wei, L. Zhang, Z.-K. Hu, S.-Y. Tang, and X.-K. Gao, "An advanced broadband absorptive balun for modern communication systems," *IEEE Trans. Circuits Syst. II, Exp. Briefs*, early access, 2024, doi: 10.1109/TCSII.2024.3372637.

[6] X. Shi, Y. Xue, Y.-J. Yang, and J.-X. Chen, "A wideband DRWG balun with low loss and compact size," *IEEE Microw. Wireless Technol. Lett.*, early access, 2024, doi: 10.1109/LMWT.2024.3364667.

[7] S. Muhammed, B. Obot, and K. Udofia, "Design and optimization of microstrip antenna for 5G wireless applications using genetic algorithm," *J. Eng. Res. Rep.*, vol. 26, no. 9, pp. 323–337, 2024, doi: 10.9734/JERR/2024/v26i91284.

[8] X. Zhang, Y. Hu, and A. Zhan, "Design of a new balanced side-slotted Vivaldi antenna with director using genetic algorithm," *Appl. Comput. Electromagn. Soc. J.*, vol. 39, no. 11, pp. 886–894, 2024, doi: 10.13052/2023.ACES.J.381107.

[9] R. Bichara, F. Asadallah, M. Awad, and J. Costantine, "Quantum genetic algorithm for the design of miniaturized and reconfigurable IoT antennas," *IEEE Trans. Antennas Propag.*, vol. 71, no. 6, pp. 1–10, 2023, doi: 10.1109/TAP.2023.3245199.

[10] B. Ezzahry, T.-E. Elhamadi, M. Lamsalli, and N. Touhami, "New method based on genetic algorithm and Minkowski fractal for multiband antenna designs," *Int. J. Microw. Wireless Technol.*, vol. 16, pp. 1–12, 2024, doi: 10.1017/S1759078723001071.

[11] S. D. Rogers, *Genetic Algorithm Optimization and Realization of Broadband Wire Monopoles*, Ph.D. dissertation, Dept. Electr. Eng., Clemson Univ., Clemson, SC, USA, 2000.

[12] S. D. Rogers, C. M. Butler, and A. Q. Martin, "Realization of genetic algorithm-optimized wire antenna with 5:1 bandwidth," *Radio Sci.*, vol. 36, no. 6, pp. 1315–1325, Nov.–Dec. 2001, doi:10.1029/2000RS002611.

[13] S. D. Rogers, C. M. Butler, and A. Q. Martin, "Design and realization of GA-optimized wire monopole and matching network with 20:1 bandwidth," *IEEE Trans. Antennas Propag.*,

vol. 51, no. 3, pp. 493–502, Mar. 2003, doi: 10.2528/PIERM09012204

[14] X. Ding, B. -Z. Wang, G. Zheng and X. -M. Li, "Design and Realization of a GA-Optimized VHF/UHF Antenna With "On-Body" Matching Network," in IEEE Antennas and Wireless Propagation Letters, vol. 9, pp. 303-306, 2010, doi: 10.1109/LAWP.2010.2047374.

[15] S. Chakravarty, R. Mittra, and N. R. Williams, "Application of micro-genetic algorithm (MGA) to the synthesis of broadband microwave absorbers comprising multiple frequency selective surfaces embedded in dielectric and magnetic media," in *Proc. IEEE Antennas Propag. Soc. Int. Symp. (APSURSI)*, Boston, MA, USA, 2001, vol. 4, pp. 692–695, doi: 10.1109/APS.2001.959560.

[16] K. Yegin and A. Q. Martin, "On the design of broad-band loaded wire antennas using the simplified real frequency technique and a genetic algorithm," *IEEE Transactions on Antennas and Propagation*, vol. 51, no. 2, pp. 220-228, Feb. 2003, doi: 10.1109/TAP.2003.809056.

[17] Z. Cheraiet, M. T. Benhabiles, and M. L. Raiabi, "Interwound and concentric 1:4 transmission line transformer using coupled microstrip lines," in *Proc. IEEE MTT-S Int. Conf. Numer. Electromagn. Multiphys. Model. Optim. RF, Microw., Terahertz Appl. (NEMO)*, 2017, doi: 10.1109/NEMO.2017.7964204.

[18] G. Guanella, "New method of impedance matching in radio-frequency circuits," *Brown Boveri Rev.*, vol. 31, no. 9, pp. 327–329, Sep. 1944.

[19] C. L. Ruthroff, "Some broad-band transformers," *Proc. IRE*, vol. 47, no. 8, pp. 1337–1342, Aug. 1959, doi: 10.1109/JRPROC.1959.287200.

[20] S. C. Dutta Roy, "Optimum design of exponential line transformer for wide band matching at low frequencies," *Proc. IEEE*, vol. 67, no. 11, pp. 1563–1564, Nov. 1979, doi: 10.1109/PROC.1979.11517

[21] J. Sevick, *Design and Realization of Broadband Transmission Line Matching Transformers*. Norwood, MA, USA: Artech House, 1989.

[22] T. Badriyah, F. Setyorini, and N. Yuliawan, "The implementation of genetic algorithm and routing Lee for PCB design optimization," in *Proc. Int. Conf. Informatics Comput. (ICIC)*, 2016, pp. 148–153, doi: 10.1109/IAC.2016.7905706.

[23] A. Boag, E. Michielssen, and R. Mittra, "Design of electrically loaded wire antennas using genetic algorithms," *IEEE Trans. Antennas Propag.*, vol. 44, no. 5, pp. 687–695, May 1996, doi: 10.1109/8.496255.

[24] Z. Altman, R. Mittra, and A. Boag, "New designs of ultra-wide-band communication antennas using a genetic algorithm," *IEEE Trans. Antennas Propag.*, vol. 45, no. 10, pp. 1494–1501, Oct. 1997, doi: 10.1109/8.633856.

[25] M. Bod, M. A. Boroujeni, and K. M. Aghdam, "Broadband loaded monopole antenna with a novel on-body matching network," *AEU—Int. J. Electron. Commun.*, vol. 70, no. 11, pp. 1551–1555, Nov. 2016, https://doi.org/10.1016/j.aeue.2016.09.012

[26] M. Bod, M. Ahmadi-Boroujeni, and K. Mohammadpour-Aghdam, "Design of a low-cost broadband loaded dipole antenna for VHF/UHF frequency range," *IET Microw. Antennas Propag.*, vol. 13, no. 12, pp. 1983–1988, Oct. 2019, doi: 10.1049/iet-map.2018.5753.

[27] P. L. Werner and D. H. Werner, "Design synthesis of miniature multiband monopole antennas with application to ground-based and vehicular communication systems," *IEEE Antennas Wireless Propag. Lett.*, vol. 4, pp. 104–106, 2005, doi: 10.1109/LAWP.2005.846169.

[28] Y. Hong, S. Kwong, Q. S. Ren, and X. Wang, "A comprehensive comparison between real population-based tournament selection and virtual population-based tournament selection," in *Proc. IEEE Congr. Evol. Comput. (CEC)*, 2007, pp. 445–452, doi: 10.1109/CEC.2007.4424505

[29] A. D. Johnson, J. A. Caripidis, and S. B. Venkatakrishnan, "Deployable inverted-hat monopole with 3:1 constant gain bandwidth," *IEEE Antennas Wireless Propag. Lett.*, vol. 19, no. 6, pp. 935–938, Jun. 2020, doi: 10.1109/LAWP.2020.2983746.

[30] D. Qin and B. Sun, "VHF/UHF wideband slim monopole antenna with distributed matching structures," *Int. J. Antennas Propag.*, vol. 2022, Art. no. 3369422, pp. 1–13, 2022, https://doi.org/10.1155/2022/3369422

[31] P. Sindhuja, "Automatic optimization of antenna using the Pareto genetic algorithm," M.S. thesis, Shizuoka Univ., Shizuoka, Japan, 2015.

[32] H. Li, T. Zheng, Y. Mao, and Y. Zhou, "A miniaturized pattern-reconfigurable antenna for broadband VHF and UHF communications," *Applied Computational Electromagnetic Society Journal.*, vol. 39, no. 8, pp. 668–674, Aug. 2024, https://doi.org/10.13052/2024.ACES.J.390801

[33] J. Choi, F. T. Dagefu, B. M. Sadler, and K. Sarabandi, "A miniature actively matched antenna for power-efficient and bandwidth-enhanced operation at low VHF," *IEEE Trans. Antennas Propag.*, vol. 69, no. 1, pp. 556–561, Jan. 2021, doi: 10.1109/TAP.2020.3004990.

[34] D. Qin, B. Sun, and R. Zhang, "VHF/UHF ultrawideband slim monopole antenna with parasitic loadings," *IEEE Antennas Wireless Propag. Lett.*, vol. 21, no. 10, pp. 2050–2054, Oct. 2022, doi: 10.1109/LAWP.2022.3190015.

[35] X. H. Zhang, X. W. Dai, W. Sun, H. Jin, and G. Q. Luo, "Sleeve monopole antenna with choke structure for broadband application," *IEEE Antennas Wireless Propag. Lett.*, vol. 20, no. 7, pp. 1230–1233, Jul. 2021, doi: 10.1109/LAWP.2021.3076049.

[36] A.-S. Kaddour, S. Bories, A. Bellion, and C. Delaveaud, "Frequency reconfigurable low-profile UWB magneto-electric dipole in VHF band," *IEEE Access*, vol. 9, pp. 61269–61282, 2021, doi: 10.1109/ACCESS.2021.3073094.

[37] B. Tütüncü, "Compact low radar cross-section microstrip patch antenna using particle swarm optimization," *Microw. Opt. Technol. Lett.*, vol. 61, no. 10, pp. 2288–2294, Oct. 2019, doi: 10.1002/mop.31893.

[38] B. Tütüncü and M. Kösem, "Substrate Analysis on the Design of Wide-Band Antenna for Sub-6 GHz 5G Communication," *Wireless Personal Communications*, vol. 125, no. 2, pp. 1523–1535, Jul. 2022, doi: 10.1007/s11277-022-09619-9.

[39] Raveendra, Muddineni, Sreelakshmy, R., Sindhuja, N. M. Mary, Florin Raja Singh, R., Chiu, Chien-Wen, Kumar, Om Prakash, Design of a Broadband Monopole Whip Antenna on an Electrically Small Ground Plane for Long Distance Radio Communications Using Genetic Algorithm, *International Journal of Antennas and Propagation*, 2026, 9034410, 15 pages, 2026. https://doi.org/10.1155/ijap/9034410



Muddineni Raveendra received the B.Tech. degree in Electronics and Communication Engineering from Vel Tech University, Chennai, India, in 2020 and the M.S. degree in Electronic Engineering from National Ilan University, Taiwan, in 2022. During his under graduation, he was awarded the Vel Tech Mahatma Gandhi National Merit Scholarship for four consecutive years. In 2020, he joined the Secure Wireless Communication Laboratory, National Chin-Yi University of Technology, Taiwan, as a Research Intern under the Taiwan Experience Education Program. During his master course he did research on broadband antennas for handheld radio communication systems with Unication Co., Ltd., Taiwan. He then joined Rapidtek Technology Inc., Taiwan as an Antenna Engineer developing Ku-band satellite antennas and RF filters. In 2023, he joined Sercomm Corporation, Taiwan as an RF Hardware Design Engineer to work on Wi-Fi 7 antenna systems. Since December 2025, he has been a Senior RF Hardware Design Engineer in Foxconn, Hsinchu, Taiwan, focusing on MIMO antenna systems and RF integration for next generation wireless communication equipment. His research interests include broadband and multiband antennas, microwave passive circuits, antenna optimization using genetic algorithms, and antenna isolation enhancement. He has published many journal papers, IEEE conference papers and book chapters. He is Academic Editor for IET Circuits, Devices & Systems and reviewer for international scientific journals.



Chien-Wen Chiu received his B.S. degree from National Taiwan Normal University, Taipei, Taiwan, in 1984, and his M.S. and Ph.D. degrees in Electrical Engineering from National Taiwan University, Taipei, Taiwan, in 1990 and 1996, respectively. He is currently a Professor in the Department of Electronic Engineering at National Ilan University, Ilan City, Taiwan. Throughout his research career, Dr. Chiu has published over 40 SCI-indexed journal papers, including articles in prestigious journals such as the *IEEE Transactions on Antennas and Propagation*. He has also served as a reviewer for numerous IEEE journals in the areas of antennas, electromagnetic wave theory, and related applications. His current research interests include AIoT (Artificial Intelligence of Things) applications, ultra-wideband antenna design, and microwave radiometer systems.



C. Kohila is an accomplished academician serving as an Assistant Professor in the Department of Electronics and Communication Engineering at PSNA College of Engineering and Technology (Autonomous), Dindigul, Tamil Nadu, India. With a strong commitment to teaching and research, she has been actively involved in shaping the academic and professional growth of engineering students. Her expertise spans key areas such as Environmental Sustainability, Signal Processing, and Antenna Design, where she integrates theoretical knowledge with practical applications.



Saravanakumar U. is a Professor and Head of Department of Electronics and Communication Engineering at Muthayammal Engineering College (Autonomous), Namakkal. He received his B.E (ECE), M.E (VLSI Design) and PhD (ICE) in 2006, 2008 and 2014 respectively. His research interests include VLSI Design, Embedded Systems and Silicon Photonics. Much of his work has been on improving the understanding, design, and performance of on chip communication, mainly through the application of network concept in to System on Chip. Dr Saravanakumar is an editor of *Advances in Intelligent Systems* (Springer) and is the author of over forty papers on VLSI and Silicon Photonics. He is an editorial board member of International Journal of Electronics, Communications, and Measurement Engineering (IJECME) (IGI Global Publishers) and American Journal of Electrical and Computer Engineering (Science Publishing Group, USA).